Available online at www.sciencedirect.com
ScienceDirect
ELSEVIER
Deep-Sea Research II 53 (2006) 2095–2113
DEEP-SEA RESEARCH PART II
www.elsevier.com/locate/dsr2

Phytoplankton processes during a mesoscale iron enrichment in the NE subarctic Pacific: Part I—Biomass and assemblage

Adrian Marchetti[a,*], Nelson D. Sherry[b], Hiroshi Kiyosawa[c], Atsushi Tsuda[d], Paul J. Harrison[e]

[a]*Department of Botany, University of British Columbia, 6270 University Blvd, Vancouver B.C., Canada V6T 1Z4*
[b]*Department of Earth and Ocean Sciences, University of British Columbia, 6270 University Blvd, Vancouver B.C., Canada V6T 1Z4*
[c]*Marine Biological Research Institute of Japan, 4-3-16 Yutaka-cho., Shinagawa-ku, Tokyo 142-0042, Japan*
[d]*Ocean Research Institute, University of Tokyo, Nakano, Tokyo 164-8639, Japan*
[e]*Atmosphere, Marine and Coastal Environment Program, Hong Kong University of Science and Technology, Clear Water Bay, Hong Kong, China*

Received 14 September 2004; accepted 6 May 2006
Available online 12 October 2006

Abstract

We report results from the Subarctic Ecosystem Response to Iron Enrichment Study (SERIES) experiment in waters of the NE subarctic Pacific in which a large scale iron (Fe) enrichment lead to a shift in the phytoplankton assemblage from pico- and nanophytoplankton to one dominated by large diatoms. The phytoplankton response to the added Fe was monitored for 26 days following two infusions into a 77 km^2 patch of seawater. During the course of the experiment, the resulting algal bloom was constrained within the upper 30 m and spread to a region measuring over 1000 km^2. Phytoplankton chlorophyll *a* (chl *a*) increased from 0.3 mg m^{-3} to a peak of 6.3 mg m^{-3} 18 days after the initial addition of Fe. Water-column integrated chl *a* was enhanced 8-fold, reaching a maximum of 114 mg m^{-2} on day 17. The resulting bloom is described in two ecological phases based on dominant phytoplankton groups. In Phase I, which encompassed the initial infusion up to day 10, all size-fractions (0.2–2, 2–20 and >20 μm) increased in biomass as indicated by chl *a*, contributing to a surface standing stock of 2 mg m^{-3}. In Phase II, from days 10 to 18, the bloom was dominated by microphytoplankton (>20 μm), with a concomitant decrease in phytoplankton <20 μm. Microphytoplankton, which initially accounted for 25% of the phytoplankton biomass and increased by a factor of 50, consisted primarily of the pennate diatom genera, *Pseudo-nitzschia, Neodenticula* and *Thalassiothrix* and the centric diatom genera, *Chaetoceros*, *Rhizosolenia,* and *Proboscia*. Particulate carbon-to-chl *a* (PC: chl *a*) ratios for large cells ($\geqslant 5$ μm) decreased 5-fold by day 18, indicative of enhanced cellular chl *a* content and increased phytoplankton contributions to PC. Pennate diatoms were most abundant in the patch, although when converted to biovolume, centric diatoms contributed larger amounts of algal carbon (C) to the bloom. A rapid decline in chl *a* on day 19 marked the onset of bloom decline. The magnitude, duration and composition of the phytoplankton response to the Fe enrichment clearly depicted a major shift in the structure of the algal assemblage and increased C export potential.

Keywords: Fe enrichment; NE subarctic Pacific; chlorophyll *a*; Phytoplankton; Diatoms; Carbon-to-chlorophyll ratios

*Corresponding author. School of Oceanography, University of Washington, Box 357940, Seattle, WA 98195, USA. Tel.: +1 206 221 7841; fax: +1 206 543 6073.
E-mail address: amarchetti@ocean.washington.edu (A. Marchetti).

0967-0645/$ - see front matter © 2006 Elsevier Ltd. All rights reserved.
doi:10.1016/j.dsr2.2006.05.038

1. Introduction

Initial support for the Fe hypothesis was obtained from shipboard bottle experiments performed in the NE subarctic Pacific (Martin and Fitzwater, 1988; Martin et al., 1989, 1990; Coale, 1991). Iron additions resulted in enhanced phytoplankton growth, providing compelling evidence that algal biomass was primarily regulated by its availability. Since then, considerable advances have been made in our understanding of the extent to which phytoplankton are limited by Fe and the essential role that this trace element performs in cellular processes.

The Fe hypothesis was first proposed to explain the paradox within regions where macronutrients, such as nitrate (NO_3), silicic acid ($Si(OH)_4$) and phosphate (PO_4), were plentiful, but phytoplankton biomass remained comparatively low throughout the year (high-nutrient, low-chlorophyll regions; HNLC). The levels of dissolved Fe in these waters are in subnanomolar concentrations, which limits phytoplankton growth and results in incomplete macronutrient utilization (Martin et al., 1991; Johnson et al., 1997; Fung et al., 2000). These ecosystems are dominated by certain phytoplankton taxa that are more competitive under low Fe conditions due to their high surface area-to-volume ratios and their ability to implement low Fe-requiring metabolic pathways (Sunda et al., 1991; Sunda and Huntsman, 1995, 1997). Though ubiquitously present, larger phytoplankton such as diatoms are generally unable to flourish under these low ambient Fe concentrations and only maintain minimal seed populations.

The ambient phytoplankton assemblage in the NE subarctic Pacific is primarily composed of small ($<5\,\mu m$) flagellates (Booth et al., 1993; Boyd and Harrison, 1999). Diatoms and other large phytoplankton usually comprise between 10% and 30% of total chl *a* (Boyd et al., 1996; Boyd and Harrison, 1999). However, over the duration of a typical summer, dissolved NO_3 and $Si(OH)_4$ are utilized, resulting in a $Si(OH)_4$: NO_3 drawdown ratio of ca. 1.6:1 (Whitney and Freeland, 1999). Within the Gulf of Alaska, surface depletion of $Si(OH)_4$ has also occasionally been observed (Wong and Matear, 1999; Whitney et al., 2005). Thus silicon-requiring diatoms contribute significantly to seasonal nutrient consumption. External sources of Fe required to stimulate growth of these diatom populations are speculated to be sporadic and spatially patchy, either from slow-moving eddies transporting Fe from coastal regions (Johnson et al., 2005) or from dust and wildfire atmospheric deposition (Boyd et al., 1998; Bishop et al., 2002). Therefore, it appears that episodic Fe additions and subsequent increases in phytoplankton growth are a naturally occurring phenomenon in the NE subarctic Pacific.

To date, there have been numerous mesoscale Fe enrichment studies in the Equatorial Pacific (IronEx I, Martin et al., 1994; IronEx II, Coale et al., 1996), Southern Ocean (SOIREE, Boyd et al., 2000; EisenEx, Gervais et al., 2002 and SoFeX; Coale et al., 2004) and the subarctic NW Pacific (SEEDS, Tsuda et al., 2003). All Fe enrichment experiments were performed with common objectives in an attempt to test the Fe hypothesis. These objectives include the documentation and quantification of the system response to Fe enrichment and to verify the extent of C sequestration coinciding with the increase in phytoplankton biomass. Although comparable trends have been observed among Fe enrichments performed in different HNLC regions, the range in Fe-induced bloom longevities and shifts in phytoplankton composition demonstrate considerable variability in the ecosystem responses. The NE subarctic Pacific was the last of the three major HNLC regions where an in situ Fe enrichment experiment had yet to be performed. The region's unique physical and biological properties necessitate an understanding of the geochemical, physiological and ecological responses to Fe enrichment.

In July 2002, a mesoscale Fe addition experiment, Subarctic Ecosystem Response to Iron Enrichment Study (SERIES), was performed in the NE subarctic Pacific. Here we report on the spatial and temporal dynamics in phytoplankton biomass as inferred by chl *a* throughout the bloom. We quantify the algal biomass incorporated into pico-, nano-, and microphytoplankton size-classes by size-fractionated chl *a*. Changes in particulate carbon (PC) are also reported along with the resulting PC: chl *a* ratios. Lastly, a detailed assessment of phytoplankton taxa in the Fe-enriched patch is given as well as estimates of C export potential for the major diatom species composing the bloom. In two companion papers, we describe the phytoplankton nutrient utilization dynamics and changes in primary productivity throughout the mesoscale Fe enrichment (Marchetti et al., this issue-a; Marchetti et al., this issue-b).

2. Materials and methods

2.1. SERIES: design and sampling strategy

The SERIES experiment was conducted from July 9 to August 4, 2002, and involved the addition of dissolved $FeSO_4$ to a 77 km^2 patch of seawater located at 144.45°W, 50.20°N, NW of Ocean Station Papa (OSP) in the NE subarctic Pacific Ocean. Complete details of site selection criteria and methods for the Fe infusion are described in Law et al. (this issue). In brief, Fe in the form of $FeSO_4$ was dissolved in seawater and added to surface waters along with the inert tracer gas, sulfur hexafluoride (SF_6). The Fe-enriched waters (referred to as the IN-patch) were mapped nightly using the SF_6 tracer along with surface chl *a* and NO_3 concentrations in the later stages of the bloom. For each day, the bottom of the patch or trace layer depth (z_{tl}) was determined as the depth at which the SF_6 concentration decreased to 50% of the average upper mixed layer SF_6 concentration. After the initial Fe infusion, dissolved Fe concentrations reached a maximum of ca. 2 nM relative to initial Fe concentrations of <0.1 nM (Boyd et al., 2004). On day 7, a second Fe infusion ($FeSO_4$ only) was performed in the center of the aging patch because dissolved Fe concentrations had returned to low levels. Sampling of the IN-patch center (determined by SF_6 local maxima), commenced on day 2 of the experiment and was performed daily between 6:00 and 10:00 Pacific Standard Time (PST). On days 1, 6, 11, 16 and 19, control stations (referred to as the OUT-patch) were sampled in adjacent waters outside of the patch. Due to ship logistics, the location of the OUT-patch stations with reference to the center of the IN-patch varied between sampling days. Day 1 of the SERIES experiment was defined as the 24-h period starting on July 10 (PST).

Vertical profiles of water-column physical structure were collected using a General Oceanics MK3C/WOCE CTD. Upper mixed layer depths (z_{uml}) were estimated from CTD data as the depth at which the change in $\sigma_T \geqslant 0.02\ m^{-1}$. To determine the photosynthetically active radiation (PAR, 400–700 nm), downwelling irradiance was measured at depth at 13 specific wavelength channels using a Satlantic SeaWifs Profiling Multichannel Radiometer. To correct for changes in incident irradiance (I_o) during the profile, incident downwelling irradiance just above the ocean surface was measured concurrently for the same 13 wavelengths using a Satlantic Ocean Radiometer. PAR (mol quanta $m^{-2}\ d^{-1}$) was integrated over the wavelengths ranging from 400 to 700 nm.

For estimates of phytoplankton biomass, discrete samples of seawater were collected with 10 L Niskin-type bottles mounted on a rosette frame. Samples were obtained at six depths corresponding to ca. 100% (surface), 33%, 10%, 3%, 1% and 0.1% of I_o. Samples below the euphotic depth ($<1\%\ I_o$) were taken to ensure the collection of water below the patch throughout the experiment. All samples were dispensed immediately and gently into distilled water-rinsed brown polyethylene bottles via silicone tubing. At each sampling depth, two Niskin bottles were triggered to ensure true replicates were obtained. For variables where triplicate measurements were performed, two samples were taken from one bottle and one from the second bottle.

2.2. Patch transects

On days 15 and 19, samples were taken on overnight transects of the Fe-enriched waters to determine spatial variability of surface chl *a* and NO_3 concentrations. In this paper, only chl *a* data from day 19 are presented. For these surveys, all variables were measured from samples obtained by shipboard flow-through seawater collected from a maximum depth of 3 m below the bow of the ship. Surface water fluorescence was measured by a Wetlabs Wetstar flow-through fluorometer calibrated with discrete samples collected throughout the patch and measured by extracted chl *a* methods described below.

2.3. Size-fractionated chlorophyll a

To estimate size-fractionated chl *a*, 300 ml of seawater was filtered gently in triplicate by gravity through 20 and 5 μm pore size (47 mm) polycarbonate filters and with an in-line vacuum (<100 mmHg) through 2 and 0.2 μm pore size (47 mm) polycarbonate filters using a filter cascade. Filters were rinsed with particulate-free seawater and immediately frozen at −20 °C until analysis onshore. The chl *a* content of the frozen samples was determined by extraction in 90% acetone at −20 °C for 24 h and measured by in vitro fluorometry using a Turner Designs 10-AU fluorometer. Chl *a* size-classes are separated into picophytoplankton (0.2–2 μm), nanophytoplankton (2–20 μm,

through the summation of 2 and 5 μm filters) and microphytoplankton (>20 μm). For some data analyses, phytoplankton size structure was further simplified into <5 μm and ⩾5 μm size-classes by combining measurements from the 0.2 and 2 μm filters (<5 μm) and the 5 and 20 μm filters (⩾5 μm). Water-column integrated chl *a* was calculated down to the 1% I_o depth through trapezoidal integration.

2.4. Size-fractionated particulate carbon

Size-fractionated PC was measured by collecting at least 1 L of seawater from the surface sampling depth (ca. 100% I_o, 2–5 m). Samples were filtered gently by gravity onto polycarbonate filters (5 μm pore size) and vacuum (<100 mmHg) onto glass fibre filters (0.7 μm nominal pore size, pre-combusted at 450 °C for 4.5 h) using a filter cascade. Particulates collected on the polycarbonate filter were then rinsed onto a glass fibre filter using an artificial saline solution to minimize particulate C contamination. Filters were oven-dried at 50 °C for 24 h and stored in a desiccator until onshore analysis. Elemental C was measured using a Carlo Erba 1106 elemental analyzer.

2.5. Phytoplankton enumeration and diatom carbon quotas

For autotrophic prokaryotes and flagellates, 300 ml of seawater was preserved with 1% glutaraldehyde and for diatoms and other larger phytoplankton, ca. 1 L of seawater was preserved with 2% borax-buffered formalin in white polyethylene bottles. Microscope slides were added to each of the 1 L bottles to reduce the dissolution rate of diatom frustules. Preserved samples were placed in the dark at 4 °C until onshore analysis. In the laboratory, picophytoplankton and nanophytoplankton were enumerated by filtering subsamples of 1–100 ml of preserved seawater onto black Nuclepore filters (1 μm pore size) and stained with DAPI and FITC. Counts were performed using an epifluorescence microscope. For larger phytoplankton species, 50–100 ml aliquots of preserved seawater were settled for 24 h in Utermöhl settling chambers and enumerated using an inverted microscope.

To estimate diatom C quotas, whole-water samples were collected in duplicate 250 ml dark glass bottles and preserved with 5% borax-buffered formalin. Determination of cell size of the dominant diatom species was performed using scanning electron microscopy (SEM) and light microscopy. For SEM preparation, an aliquot of preserved cells was settled for 24 h and concentrated to 5 ml. The concentrated material was acid-cleaned and filtered onto a polycarbonate filter (1 μm pore size) according to methods described by Hasle and Fryxell (1970). Filters were dried and mounted onto aluminum stubs, coated with Au–Pd and examined using a Hitachi S-4700 field emission SEM. Cell volumes were estimated from the SEM images of 4–10 cells for each selected genus or species and by assuming that pennate diatoms have a rectangular prism shape ($V_p = L \times W \times H$) and centric diatoms have a cylindrical shape ($V_c = \Pi r^2 \times H$). C content for each diatom genus was then estimated from average cell volume using the conversion factor provided in Montagnes et al. (1994).

3. Results

3.1. Mixed layer properties

The first Fe release resulting in an initial dissolved Fe concentration of ca. 2 nM was conducted in waters with an uncommonly shallow upper mixed layer depth (z_{uml}) of ca. 10 m (Fig. 1). Average summer z_{uml} at OSP are generally between 30 and 40 m (Whitney and Freeland, 1999). On day 5, an increase in mixing resulted in a deepening of z_{uml} to 30 m. At this time, the IN-patch Fe concentration was reduced, necessitating a second Fe infusion on day 7 which resulted in an increase in the dissolved Fe concentration to 0.6 nM (Boyd et al., 2004). The deeper z_{uml} remained until day 8, and then shoaled to ca. 10 m. On day 12, a second strong mixing event resulted in the z_{uml} deepening to ca. 30 m. z_{uml} then remained below 20 m until day 18, after which it once again returned to above 10 m.

From the initial infusion to day 4, only the surface and 33% I_o sampling depths were positioned in IN-patch waters, as indicated by z_{tl} (Fig. 1). On day 5, the deepening of the z_{uml} and redistribution of Fe to 30 m resulted in the 10% I_o sampling depth to be included in IN-patch waters. The 1% I_o sampling depth was within the IN-patch on days 7 and 8 as a result of the deepening of z_{uml} and from day 15 onward due to the shoaling of the euphotic depth (z_{eu}) which coincided with an increase in phytoplankton biomass. The 0.1% I_o sampling depth remained below the z_{tl} for the duration of the experiment.

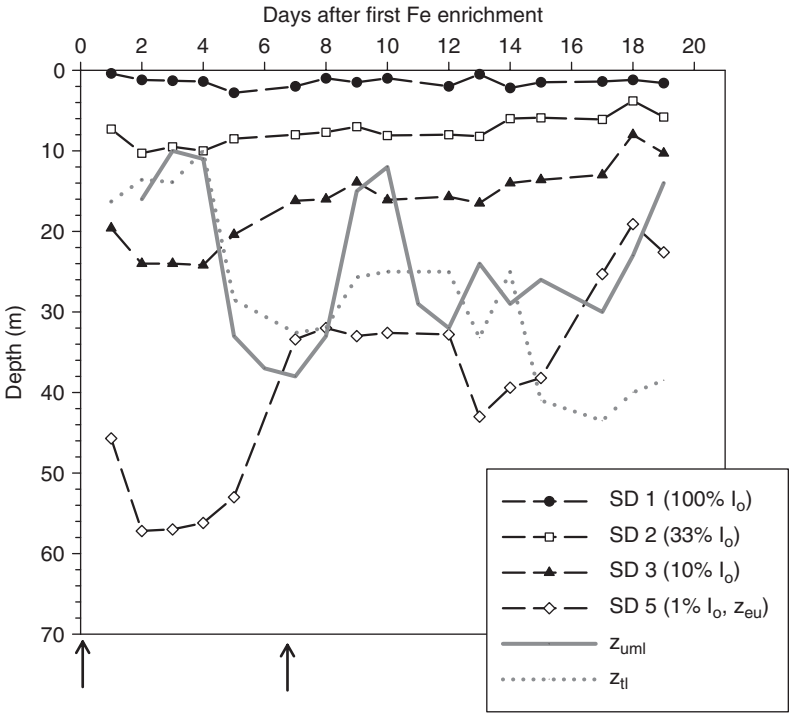

Fig. 1. Water-column sampling depths (SD) for the IN-patch throughout the Fe enrichment experiment. For reference, upper mixed layer depths (z_{uml}) and tracer layer depths (z_{tl}) are also plotted. The sampling depths shown are 4 of the 6 depths used for productivity measurements for the IN-patch and OUT-patch (3% I_o and 0.1% I_o sampling depths are not shown). The arrows indicate the days in which Fe was added to the IN-patch.

3.2. Chlorophyll *a*

Chl *a* concentrations in the ambient, pre-Fe-enriched water, were typically low, with a surface maximum of 0.3 mg m^{-3}. OUT-patch chl *a* concentrations remained relatively stable during the observation period, except on days 11–19 when slight increases were measured primarily in surface waters (Fig. 2A). At the onset of SERIES, IN-patch chl *a* concentrations doubled within 48 h of the first Fe infusion (Fig. 2B). Preceding a mixing event on day 5, the increase in chl *a* was confined to the shallow z_{uml} of 10 m. On day 5, an increase in z_{uml} resulted in a redistribution of Fe and accumulated chl *a* to 30 m. Elevated chl *a* concentrations relative to the OUT-patch were confined to above ca. 35 m throughout the remainder of the bloom, with no observed increases in chl *a* below the z_{tl}. IN-patch chl *a* concentrations were relatively uniform throughout the water-column, with variations due to sampling depths being above or below z_{uml}. On day 18, IN-patch chl *a* reached a maximum concentration of 6.3 mg m^{-3}, marking a 20-fold increase above OUT-patch chl *a* concentrations. On day 19, chl *a* concentrations decreased by 50% to <3 mg m^{-3}, signifying the onset of bloom decline.

The IN-patch changes in size-fractionated chl *a* are described in two ecological phases based on observed shifts in dominant phytoplankton size-classes. During Phase I, from the initial infusion to day 10, all size-fractions increased in chl *a* at all sampling depths in the IN-patch (Fig. 3A–D). By day 10, chl *a* concentrations had intermittently stabilized at ca. 2 mg m^{-3}, with lower chl *a* coinciding with increases in z_{uml} on days 9 and 12. During Phase II, from days 10 to 18, IN-patch chl *a* increased markedly in the microphytoplankton (>20 μm) size-class with a concomitant decrease in nanophytoplankton (2–20 μm) and picophytoplankton (0.2–2 μm) chl *a* concentrations. On days 17 and 18, microphytoplankton chl *a* concentrations peaked at 4.2 mg m^{-2}, marking a 50-fold increase in microphytoplankton chl *a* compared to the OUT-patch.

Size-fractionated, water-column integrated chl *a* followed similar trends as reported for volumetric

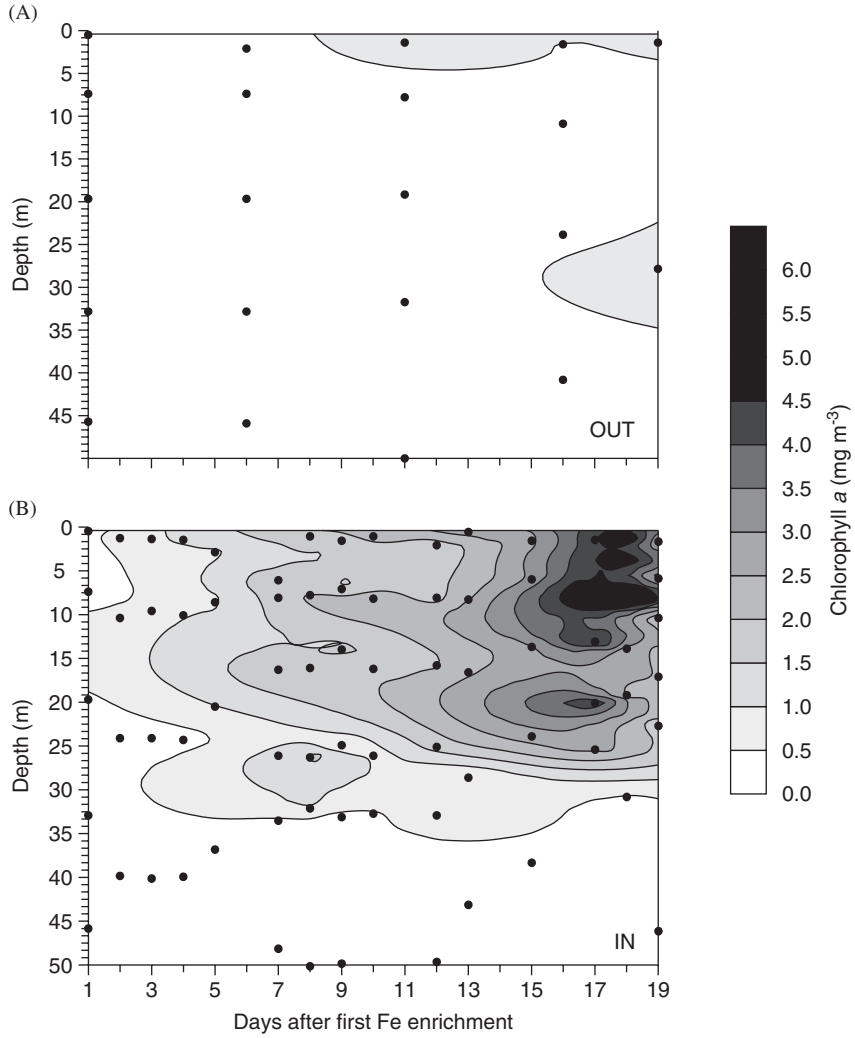

Fig. 2. Contours of chlorophyll *a* concentrations for the (A) OUT-patch and (B) IN-patch throughout the Fe enrichment experiment. Dots indicate sampling times and depths.

measurements (Table 1). In Phase I, water-column integrated chl *a* increased steadily and peaked at 60 mg m^{-2} on day 8, concurrent with high chl *a* in both picophytoplankton and nanophytoplankton. In Phase II, IN-patch microphytoplankton chl *a* steadily increased up to the peak of the bloom. Total chl *a* reached a maximum of 114 mg m^{-2} on day 17, representing an 8-fold increase compared to day 1. Water-column integrated chl *a* in the OUT-patch remained below 35 mg m^{-2} throughout the observation period (Table 1).

The OUT-patch phytoplankton assemblage was dominated by the nanophytoplankton size-class, comprising 60% of total chl *a* (Fig. 4A). Microphytoplankton and picophytoplankton contributed 20% each to total chl *a* in the ambient assemblage. The composition of OUT-patch phytoplankton size-fractions remained fairly constant, with nanophytoplankton being dominant throughout the observation period. In the IN-patch, these proportions remained constant during Phase I of the bloom (Fig. 4B). However, in Phase II, microphytoplankton comprised the majority of phytoplankton biomass, making up 86% of total chl *a* by day 17.

On day 19, spatial distributions in surface chl *a* displayed large gradients, as concentrations were higher in the center than at the periphery of the patch (Fig. 5). Peak surface concentrations of ca. 5 mg m^{-3} were confined to several isolated sections,

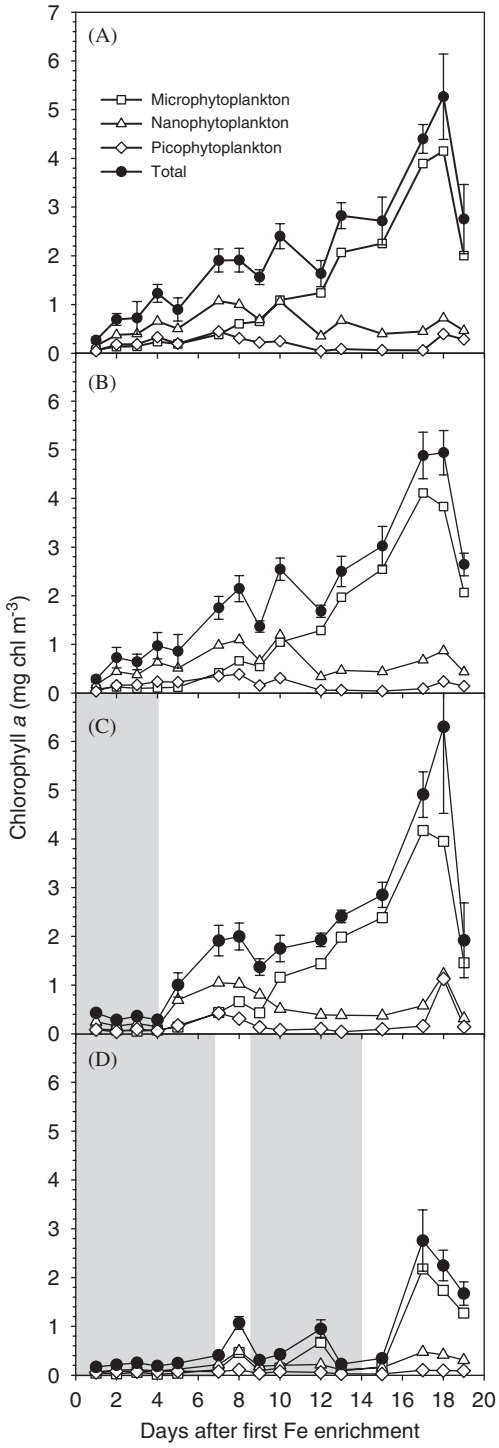

Fig. 3. Size-fractionated chlorophyll *a* concentrations in the IN-patch throughout the Fe enrichment experiment. (A) Surface (ca. 100% I_o), (B) 33% I_o, (C) 10% I_o and (D) 1% I_o sampling depths. Total chlorophyll *a* was calculated through the summation of all size-fractions. Error bars for total chlorophyll *a* represent ± 1 standard deviation associated with the mean ($n = 3$). Shaded regions indicate when sampling depths were below the Fe-enriched patch waters (as determined by z_{tl}).

constituting less than 10% of the total patch area. At this time, patch size had spread to ca. 800 km^2 and had elongated horizontally, positioned on a W–E axis.

3.3. Size-fractionated PC and PC: Chl a ratios

OUT-patch surface PC measurements ranged from 8 to 15 mmol C m^{-3} during the observation period (data not shown). IN-patch surface PC in the $\geqslant 5\,\mu m$ size-fraction increased 4-fold over the duration of the Fe enrichment and reached a maximum of 22 mmol C m^{-3} on day 19 (Fig. 6A). The $<5\,\mu m$ size-fraction PC increased slightly during Phase I of the bloom, decreased back to ambient levels on day 13, and then increased markedly leading up to bloom termination on day 19.

In the IN-patch, the initial PC: chl *a* ratio for the $\geqslant 5\,\mu m$ size-fraction was 17 mmol C (mg chl $a)^{-1}$ (Fig. 6B). During the experiment, the $\geqslant 5\,\mu m$ PC: chl *a* ratio decreased, reaching a minimum of 3.4 mmol C (mg chl $a)^{-1}$ on day 17 of the bloom. The initial PC: chl *a* ratio in the $<5\,\mu m$ size-fraction was 22 mmol C (mg chl $a)^{-1}$. This ratio decreased during Phase I of the bloom and reached a minimum of 10 mmol C (mg chl $a)^{-1}$ on day 8. During Phase II, the $<5\,\mu m$ PC: chl *a* ratio increased, surpassing the initial ratio measured for this size-fraction.

3.4. Phytoplankton assemblage and diatom carbon cellular quotas

Changes in phytoplankton species composition reflected trends observed in chl *a* throughout the Fe-enrichment experiment. During Phase I, algal taxa measured in each size-class (pico-, nano- and microphytoplankton) increased in abundance relative to the initial phytoplankton assemblage (Fig. 7 and Table 2). The cyanobacterium *Synechococcus* was the most dominant picophytoplankton whereas in the nanophytoplankton size-class, coccolithophorids were most abundant and reached a maximum density of 1×10^6 cells L^{-1} on day 10. Both Prasinophyceae and Prymnesiophyceae displayed high variability within the IN-patch and OUT-patch. In the IN-patch, a maximum Prymnesiophyceae (excluding coccolithophorids) density of 5×10^5 cell L^{-1} was also achieved on day 10. Similarly, on day 10, the dinoflagellate, *Gymnodinium* spp. reached a maximum cell density of

Table 1
Water-column integrated chlorophyll *a* ($mg\,m^{-2}$) for specific size-fractions and the total phytoplankton assemblage during SERIES

Day	Patch	Integrated Chl *a*			
		Picophytoplankton (0.2–2 μm)	Nanophytoplankton (2–20 μm)	Microphytoplankton (>20 μm)	Summed total
2	IN	5.53	12.26	4.51	22.30
3		6.00	12.98	4.16	23.14
4		7.24	15.42	5.13	27.78
5		7.56	21.77	6.05	35.38
7		10.52	28.16	12.39	51.07
8		9.45	31.06	19.59	60.09
9		3.81	18.51	12.23	34.55
10		5.25	22.47	26.32	54.04
12		2.36	11.20	41.20	54.76
13		1.79	13.91	48.75	64.45
15		2.51	12.52	75.31	90.33
17		2.48	13.87	97.27	113.62
18		8.81	15.09	58.70	82.60
19		3.79	12.12	36.39	52.30
1	OUT	2.69	7.72	3.67	14.09
6		2.20	5.00	2.13	9.33
11		2.28	8.77	5.81	16.86
16		2.58	9.36	5.79	17.73
19		2.50	12.64	18.22	33.35

Integrations are performed to the bottom of the euphotic zone (1% I_o).

4×10^4 cells L^{-1}. All other dominant autotrophic dinoflagellate populations remained $<10^3$ cells L^{-1} for the duration of the bloom. With the exception of a small centric diatom (Thalassiosiraceae) and the pennate diatoms *Cylindrotheca closterium* and *Neodenticula seminae,* initial densities of large diatom genera were $<10^3$ cells L^{-1}. Diatoms steadily increased in abundance throughout Phase I of the bloom. By day 10, the most abundant large diatoms (>10 μm) were *C. closterium*, *N. seminae*, *Pseudo-nitzschia* spp. and *Chaetoceros* spp. From days 10 to 12, a sharp decline in all non-diatom species occurred. The most marked changes were evident in *Synechococcus* spp., Prasinophyceae, Prymnesiophyceae (excluding coccolithophorids) and *Gymnodinium* spp., returning to close to pre-Fe enrichment cell densities, and coccolithophorids decreasing to 50% of their maximum attained cell density. With the exception of *C. closterium,* there were no significant decreases in large diatom populations during this period as many diatom genera continued to increase in abundance.

In Phase II of the phytoplankton bloom, excluding *Synechococcus* spp., all picophytoplankton, nanophytoplankton and dinoflagellate cell densities remained low, exhibiting only minor fluctuations between days 12 and 18. In contrast, diatom populations continuously increased, with a maximum abundance achieved on day 17, when total diatom density was estimated at ca. 3.4×10^5 cells L^{-1}. Numerically, the most dominant large diatoms were *Pseudo-nitzschia* spp., *Neodenticula* sp., and *Chaetoceros* spp. with cell densities of 2×10^5, 9×10^4 and 7×10^4 cells L^{-1}, respectively. With the exceptions of *Pseudo-nitzschia* spp., *Thalassiothrix longissima* and *Rhizosolenia hebetata*, peak cell densities of the major diatom genera were reached on day 15, with the latter genera reaching maximum abundances on days 17 or 18.

Based on increases in cell densities, net growth rates for large diatom genera were estimated. The pennate diatoms *Pseudo-nitzschia* spp. and *T. longissima* exhibited the fastest net growth rates of 0.47 and 0.41 d^{-1}, respectively (Table 3). Net growth rates of large centric diatom genera ranged between 0.20 and 0.32 d^{-1}. When converted to biovolume, the diatoms *T. longissima*, *Proboscia alata* and *R. hebetata* comprised the greatest proportions, making up 33%, 17% and 16%, respectively, of the total contributions to algal C by the major diatom species.

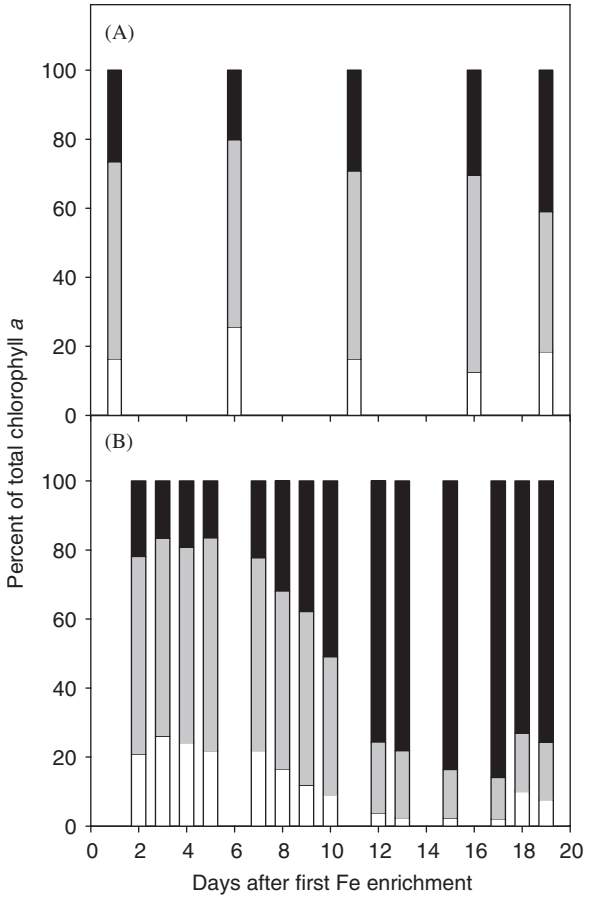

Fig. 4. Percent contributions of picophytoplankton (0.2–2 μm, white), nanophytoplankton (2–20 μm, grey) and microphytoplankton (>20 μm, black) to total chlorophyll *a* concentrations in the (A) OUT-patch and (B) IN-patch throughout the Fe enrichment experiment.

4. Discussion

4.1. SERIES algal bloom evolution

The stimulation in the growth of all phytoplankton size-classes upon Fe enrichment clearly demonstrates that phytoplankton were previously Fe-limited in this region of the NE subarctic Pacific. At the onset of the experiment, enhanced phytoplankton biomass was restricted to a shallow upper mixed layer. The large mixing event on day 5 facilitated Fe transport to ca. 30 m. Subsequent increases in phytoplankton biomass primarily took place in this 0–30 m layer for the duration of the observation period. Below the patch, Fe concentrations did not differ significantly from outside waters, likely maintaining a condition of Fe-limited phytoplankton growth. At the onset of the second ecological phase of the phytoplankton bloom, the marked decrease in small phytoplankton is speculated to be a result of extensive microzooplankton grazing. The continuous, exponential-like growth of microphytoplankton biomass throughout the bloom suggests that there was an imbalance between growth and grazing pressure in this size-class. The observations made during SERIES are consistent with the "ecumenical Fe hypothesis" (Morel et al., 1991; Price et al., 1994; Cullen, 1995), which was proposed as an expansion of the original Fe hypothesis (Martin, 1990). This hypothesis states that Fe limitation and grazing co-regulate phytoplankton growth in HNLC regions, with grazing playing a particularly significant role in regulating small cells which are often initially dominant.

Algal-specific C: chl *a* ratios at OSP are commonly observed to range between 4 and 7 mmol C (mg chl *a*)$^{-1}$ (Peña and Denman, unpubl. data). The high PC: chl *a* ratio observed in ambient waters at OSP suggests the presence of extensive amounts of non-algal associated PC. These different components of non-algal PC were not quantified, but are likely made up of heterotrophic grazers, bacteria and particulate detritus. Previous assessments of standing stocks in the NE subarctic Pacific determined that heterotrophic flagellates, bacteria and mesozooplankton could account for as much as 50% of the total PC (Boyd et al., 1995). The changes in the PC: chl *a* ratio as a result of Fe enrichment were separated between small cells (<5 μm) and large cells (≥5 μm). During Phase I (up to day 10), the PC: chl *a* ratio of small cells declined due to chl *a* concentrations increasing faster than that of PC. The minimum PC: chl *a* ratio in <5 μm cells was reached on day 8, coinciding with maximum chl *a* concentrations in the nanophytoplankton size-class. In Phase II, the PC: chl *a* ratio increased markedly due to an increase in PC, with a concurrent decrease in small cell chl *a* concentrations. Elevated non-algal <5 μm PC concentrations in the latter half of the bloom are likely the result of increases in heterotrophic bacterial abundance (Hale et al., this issue) and detritus.

In contrast, the PC: chl *a* ratio in large cells continued to decline throughout the bloom, largely due to the 20-fold increase in chl *a* concentrations, whereas PC concentrations increased only 5-fold. The uncoupling between chl *a* and PC may be attributed to known effects of Fe-limitation on cellular chl *a* content. Phytoplankton that are

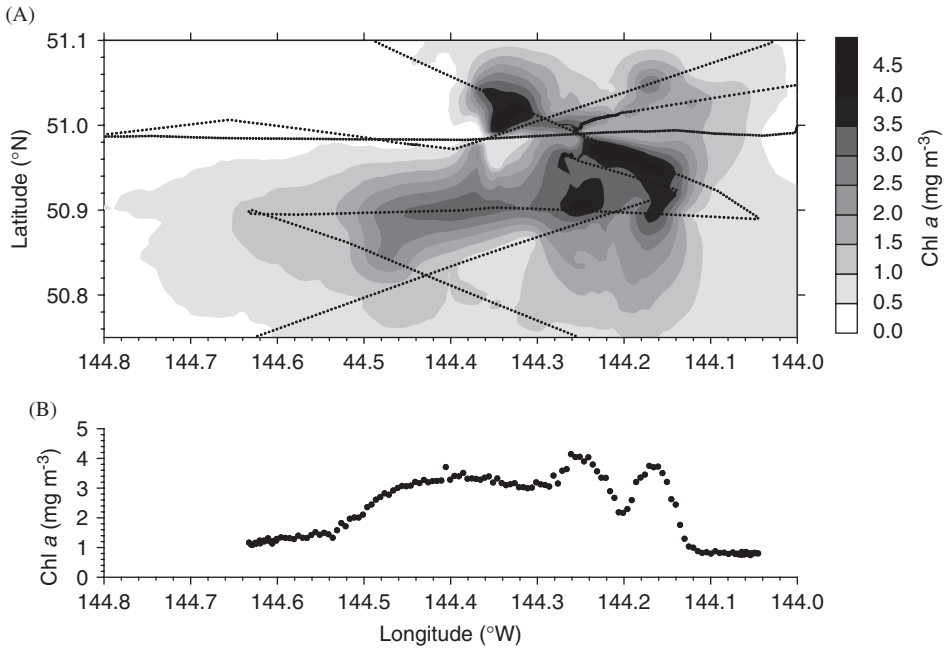

Fig. 5. (A) IN-patch spatial distributions of surface chlorophyll *a* (from in vivo fluorescence) on day 19 of the Fe enrichment experiment and (B) surface chlorophyll *a* concentrations during a transect performed along 50.9°N. The dots in (A) outline the position of the transects.

Fe-limited have reduced concentrations of cellular chl *a* (Greene et al., 1992; Geider et al., 1993). When Fe is re-supplied, phytoplankton immediately increase their cellular chl *a* concentrations along with other light-harvesting pigments. Thus, the initial response of increased chl *a* to the alleviation of Fe-stress may represent a change in phytoplankton chemical composition and physiological state rather than an increase in algal biomass. A low PC: chl *a* ratio of large cells at the peak of the bloom corroborates the observed elevation in cellular chl *a* content, and infers that phytoplankton C constituted the majority of the PC concentration.

4.2. Factors affecting phytoplankton growth and assemblage in the patch

The indigenous algal assemblage at OSP was primarily comprised of small-celled species such as *Synechoccocus*, Prymnesiophyceae (cf. *Phaeocystis* spp.), and coccolithophorids (cf. *Emiliania huxleyi*). Similarly, small pennate diatoms such as *C. closterium* and *N. seminae* and a small centric diatom belonging to Thalassiosiraceae were the most abundant diatom species. Such phytoplankters may have an advantage in low Fe waters by possessing higher surface area-to-volume ratios in comparison to their larger-sized counterparts. This allows for an increased rate of Fe uptake (proportional to cellular surface area) relative to their intracellular Fe demand (proportional to cellular volume) (Morel, 1987). Despite this advantage, the initial increase of all enumerated species in Phase I of the bloom suggests that Fe availability regulated the growth of the entire phytoplankton assemblage. In Phase II, the rapid decline of these small cells coincided with the increase in microzooplankton populations and demonstrates their greater susceptibility to grazing pressures (Rivkin, unpubl. data).

During peak chl *a* concentrations in SERIES, large pennate diatoms numerically dominated the algal bloom. Pennate diatoms have also been observed to exhibit the greatest response in other Fe enrichment experiments, particularly in IronEx II, SOIREE and SOFeX (Landry et al., 2000; Gall et al., 2001a; Coale et al., 2004). These diatoms appear to have an advantage over large centric diatoms by having faster net growth rates upon the alleviation of Fe stress. An exception was in the NW subarctic Pacific during SEEDS, where the addition of Fe resulted in a floristic shift from the initially dominant pennate diatom *Pseudo-nitzschia*

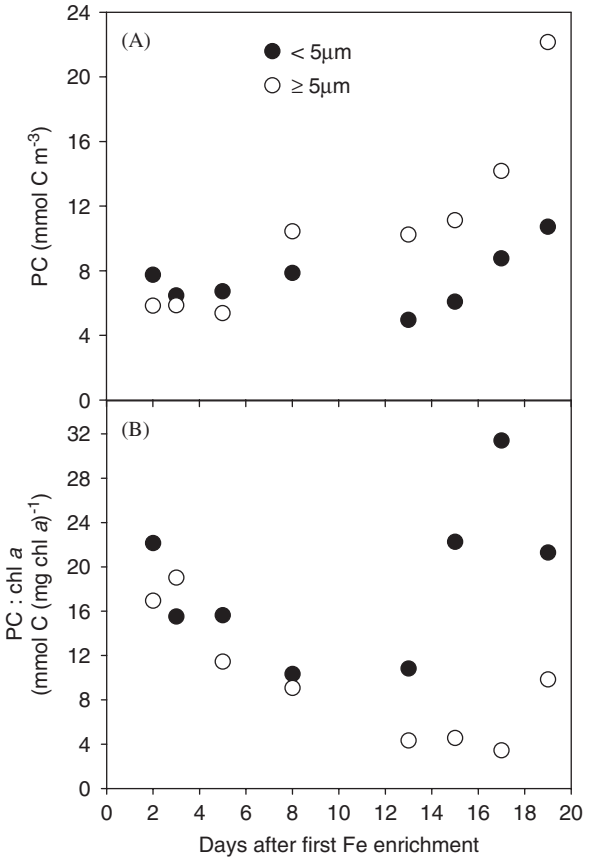

Fig. 6. Surface water (2–5 m), size-fractionated (A) particulate carbon (PC) concentrations and (B) particulate carbon-to-chlorophyll *a* (PC: chl *a*) ratios in the IN-patch during the Fe enrichment experiment.

turgidula, to the centric diatom *Chaetoceros debilis* (Tsuda et al., 2003). A shallow upper mixed layer (10–20 m) was present throughout their experimental observation period (Tsuda et al., 2005). This shallow mixed layer may have favoured the growth of certain diatoms such as *Chaetoceros* by confining the infused Fe within a thin layer of seawater at the surface where nutrients and light were abundant. In contrast, during SERIES, the initial populations of *Pseudo-nitzschia* were low when compared to *Chaetoceros*. However, by day 18, *Pseudo-nitzschia* was the most abundant diatom in the patch. Thus, although there is some consistency among HNLC regions in terms of the floristic composition of the Fe-induced algal blooms, a further understanding of the factors regulating species composition is still required.

The affinity for a specific nutrient by phytoplankton can be assessed by determining the half-saturation constant (K_s). Diatoms with high K_s values become nutrient limited at higher concentrations of a particular nutrient compared to diatoms with lower K_s values. Previous studies in the Southern Ocean have shown that the majority of K_s values for $Si(OH)_4$ uptake were between 0.7 and 10 µM, suggesting a vast range in $Si(OH)_4$ affinities for different diatom assemblages (Nelson et al., 2001). It must be noted, however, that $Si(OH)_4$ concentrations that temporarily decrease below K_s values do not necessarily lead to an immediate reduction in diatom growth rates due to their capacity to store Si in intracellular pools (Conway and Harrison, 1977). In this respect, K_μ (50% of μ_{max}), a measure of when $Si(OH)_4$ concentrations are actually growth limiting to diatoms, may be a more useful parameter to determine when diatoms are Si-limited; these concentrations are typically found to be 5–10 times lower than K_s values (Nelson and Dortch, 1996).

During SERIES, although consistent net growth rates of diatoms were observed throughout the greater part of the in situ Fe enrichment, there appeared to be two distinct groups of diatoms, distinguished by when peak populations were achieved. For certain diatoms, cell abundance peaked on day 15, whereas for others, growth continued until day 17 or 18. Intense grazing of diatoms by macrozooplankton was not evident during the phytoplankton bloom, reducing the likelihood of selective grazing pressures on diatoms (Sastri et al., this issue). Therefore, the availability of Fe and $Si(OH)_4$ in the later stages of the bloom are speculated to be the most important regulating factors to diatom growth in the patch. After day 12, dissolved Fe concentrations in the patch had decreased to pre-enrichment levels and by day 15, $Si(OH)_4$ concentrations decreased to <3 µM (Boyd et al., 2004; Marchetti et al., this issue-a). In addition, after day 12, both maximal and operational photochemical yields began to decline, marking a reduction in photosynthetic efficiency in phytoplankton (Marchetti et al., this issue-a). We hypothesize that the distinction between these two groups of diatoms may be based on their K_s values for Fe and/or $Si(OH)_4$. Diatoms which peaked in cell abundance on day 15 may have had lower affinities for Fe and/or $Si(OH)_4$ (high K_s diatoms) when compared to diatoms that continued to grow until days 17 or 18 (low K_s diatoms). To better illustrate the succession

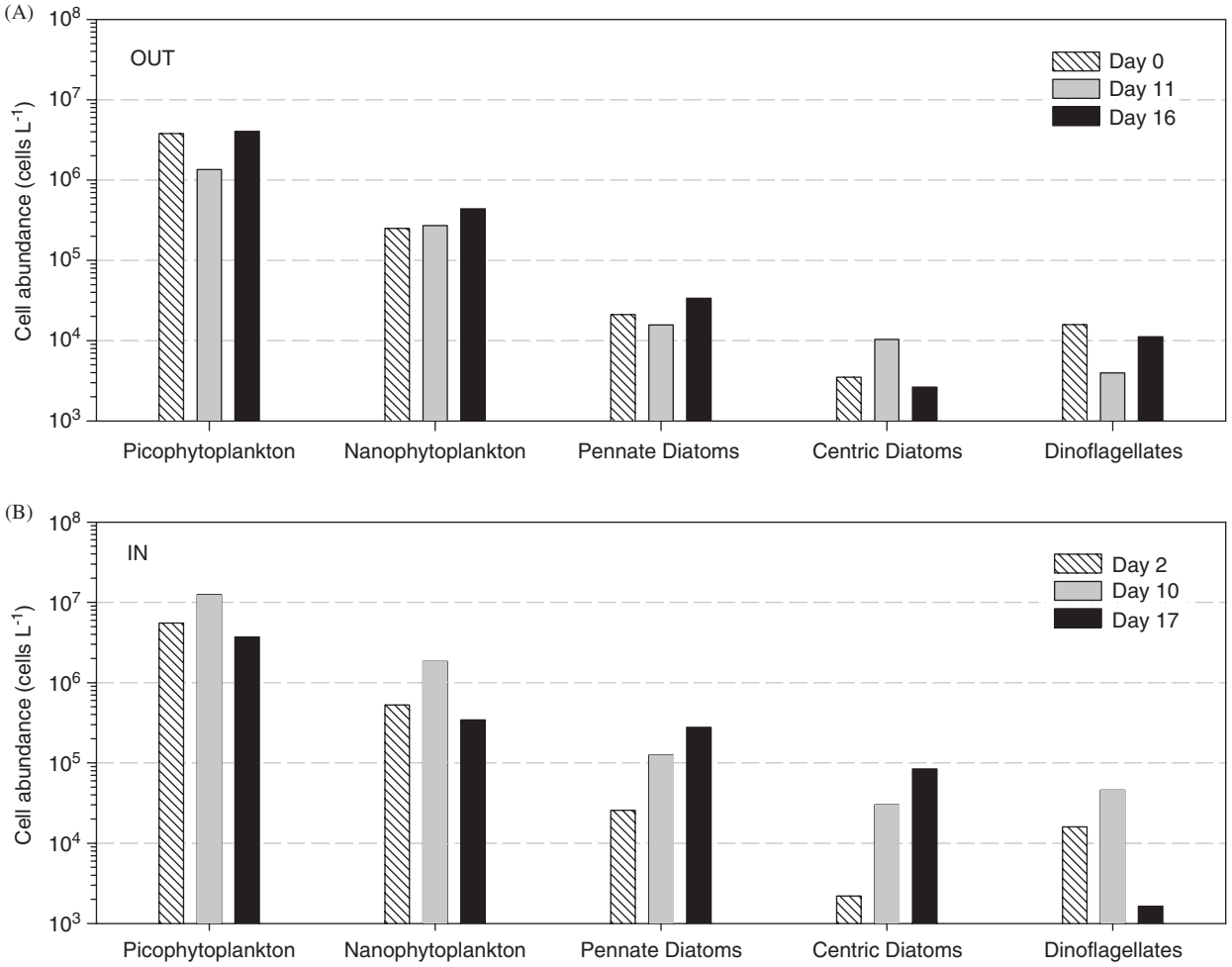

Fig. 7. Cell abundances of major phytoplankton groups in surface waters of the (A) OUT-patch and (B) IN-patch throughout the Fe enrichment experiment. *Note*: For diatoms, only >5 μm diatoms are included.

in phytoplankton throughout the bloom, we plotted representative species from each suggested group (coccolithophorids = small cells, *Chaetoceros* = large diatom with a high K_s and *Pseudo-nitzschia* = small diatom with a low K_s) with changes in concentrations of $Si(OH)_4$ and maximal photochemical yield (Φ_m), which is indicative of the degree of Fe stress (Fig. 8). Thus, decreasing Fe and/or $Si(OH)_4$ concentrations appeared to have regulated the extent of the bloom longevity and may have limited the growth of some diatoms at an earlier stage than others. A further discussion on changes in macronutrients and photosynthetic efficiency throughout the SERIES Fe enrichment is provided in Marchetti et al. (this issue-a).

4.3. Comparison of mesoscale iron enrichment experiments

With the addition of the Fe enrichment experiments recently performed in the Southern Ocean (SOFeX and EisenEx), and NW (SEEDS) and NE (SERIES) Pacific, a complete assessment of in situ phytoplankton responses to Fe for all three HNLC regions is possible (Table 4). In most experiments, the addition of Fe resulted in a phytoplankton assemblage transition from small flagellates to large diatoms. However, among regions, there are noteworthy differences in the magnitude, duration and composition of the resulting phytoplankton blooms.

The extent of the phytoplankton increase in biomass varied among regions, both in standing

Table 2
Comparison of cell abundances (cells L^{-1}) of most phytoplankton taxa at the onset, during phase I (days 0–10) and phase II (days 10–18) of SERIES

Phytoplankton taxa	Phase I			Phase I			
	Day 0	Day 5	Day 10	Day 12	Day 15	Day 17	Day 18
Picophytoplankton (0.2–2 μm)							
Synechococcus spp.	3 760 000	8 320 000	12 400 000	2 520 000	2 210 000	3 700 000	12 800 000
Chlorophyceae	29 400		114 700	36 300	141 000		35 500
Nanophytoplankton (2–20 μm)							
Cryptophyceae	3630	12 600	83 100	54 500	19 300		15 700
Prymnesiophyceae	32 700	184 400	501 200	47 200	55 900	76 300	108 000
Prasinophyceae	14 500	382 500	266 000	36 300	59 500	84 400	177 000
Coccolithophorids	200 300	380 500	984 000	479 000	74 100	183 000	81 700
Thalassiosiraceae[a]	56 700	157 000	220 000	89 000	21 000	117 000	52 400
Microphytoplankton (>20 μm)							
Diatoms							
Pseudo-nitzschia spp.	164	801	28 800	30 700	136 000	192 000	95 900
Neodenticula seminae	1920	3910	37 400	28 500	93 400	63 700	70 800
Thalassiothrix longissima	35	22	353	1060	4800	7220	12 100
Cylindrotheca closterium	18 200	30 200	43 600	3630		5450	60 500
Rhizosolenia hebetata f. *hebetata*	10	21	270	430	1500	1300	2150
Chaetoceros atlanticus	436	766	5480	7340	14 600	12 400	6070
Chaetoceros concavicornis	198	547	3720	5410	17 700	11 700	8920
Chaetoceros convolutus	484	201	9440	16 100	22 000	23 000	12 900
Chaetoceros sp.	41	320	3880	7330	14 700	6320	7080
Thalassiosira spp.	986	831	5930	4150	14 100	10 400	10 500
Proboscia alata	882	558	1380	2100	12 800	5020	7080
Total[b]	23 356	38 177	140 253	106 750	331 600	338 510	294 000
Dinoflagellates (autotrophic)							
Gymnodium spp.	14 500	33 700	43 600	14 500	14 000		10 475
Ceratium spp.	624	200	496	280	380	590	840
Protoperidinium spp.	162	54	142	120	140	200	420
Other dinoflagellates	869	513	1670	350	1070	850	450

Data are from surface waters (2–5 m) depth.
[a]Small diatom (<5 μm).
[b]Total abundances of diatoms include only listed taxa.

stocks and spatial distributions. In the Southern Ocean, chl *a* concentrations remained relatively low, $<4\,mg\,m^{-3}$. However, when chl *a* is integrated throughout the water-column, the maximum amounts in polar Fe enrichments were comparable to those observed in subpolar and tropical waters during IronEx II, SEEDS and SERIES. This is primarily a result of the deep upper mixed layers commonly present in the Southern Ocean polar regions, distributing, and possibly preventing the accumulation of high phytoplankton biomass. In contrast, the presence of shallow upper mixed layers in the North Pacific during SEEDS and SERIES resulted in rapid phytoplankton accumulation. The highest chl *a* concentrations in Fe-stimulated waters were achieved in NW subarctic waters during SEEDS, exceeding $17\,mg\,m^{-3}$. Lastly, in tropical waters, maximum phytoplankton biomass was low (ca. $3\,mg\,m^{-3}$) after alleviation of Fe stress due to lower concentrations of macronutrients and intense grazing pressure on smaller phytoplankton.

Patch longevity also varied among the Fe-induced phytoplankton blooms in each HNLC region. In Southern Ocean polar waters, enhanced phytoplankton growth appeared to be long lived. Following SOIREE, satellite imagery observed elevated chl *a* concentrations 41 days after the first Fe infusion. During IronEx II, chl *a* concentrations increased for only 7 days, whereas in SERIES, bloom decline commenced after 18 days. Variations

Table 3
Comparison of cellular abundances, net growth rates, cell volumes and carbon quotas for the major diatom genera at the onset and peak cell concentrations (days 15–18) during SERIES

Diatom	Cell abundance (cells L^{-1})		Net growth rate[c] (day^{-1})	Average cell volume[d] ($\mu m^3\,cell^{-1}$)	Average carbon quota[e] ($pmol\,C\,cell^{-1}$)	Peak total carbon ($mmol\,C\,m^{-3}$)	Relative abundance[f] (%)	Relative carbon[f] (%)
	Initial[a]	Peak[b]						
Pennate diatoms								
Pseudo-nitzschia	174	192 000	0.47	550	5	0.96	42	6
Neodenticula	2420	93 400	0.28	220	2	0.19	20	1
Cylindrotheca	18 200	60 500	NA[g]	30	0.3	0.02	13	<1
Thalassiothrix	17	12 100	0.41	45 000	409	4.95	3	33
Centric diatoms								
Chaetoceros (L)	682	40 700	0.31	5 000	45	1.85	9	12
Chaetoceros (s)	477	29 300	0.32	2000	18	0.53	6	4
Thalassiosira	986	14 100	0.20	10 500	95	1.35	3	9
Proboscia	882	12 800	0.21	22 000	200	2.56	3	17
Rhizosolenia	15	2150	0.31	125 000	1133	2.44	<1	16

Data are from the surface (2–5 m) depth of the IN-patch. L = large variety species, s = small variety species, NA = not available.
[a]Initial phytoplankton enumerations are from day 2 of the Fe enrichment experiment.
[b]Denotes maximum cell abundance achieved for the specified diatom genus.
[c]Net growth rates were calculated using cell numbers and the exponential growth equation.
[d]Cell volumes were estimated using scanning electron microscopy or light microscopy.
[e]Carbon quotas were calculated using the volume-to-carbon conversion factor outlined in Montagnes et al. (1994).
[f]Denotes the percent relative abundance and relative carbon contributions among listed diatom genera.
[g]Net growth rate could not be calculated due to fluctuations in cell abundance.

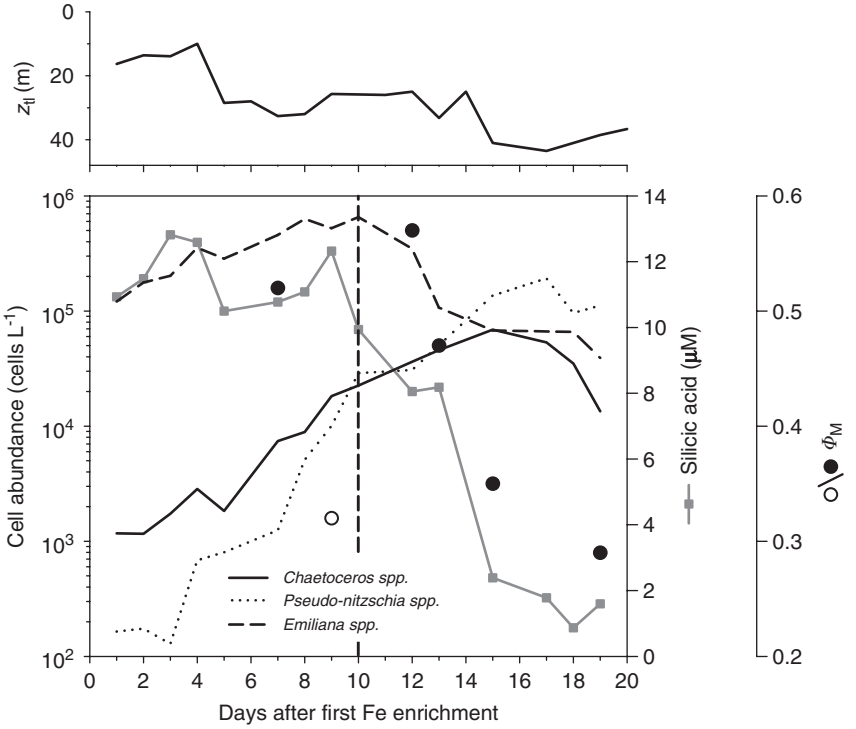

Fig. 8. Changes in cell abundances of coccolithophorids (cf. *Emiliana huxleyi*) (dashed line), *Chaetoceros* spp. (solid line) and *Pseudo-nitzschia* spp. (dotted line) during the Fe enrichment experiment. Average $Si(OH)_4$ concentrations (gray line) for the IN-patch and maximal photosynthetic yield (Φ_M) for the IN-patch (solid circles) and OUT-patch (open circles) are also plotted. The vertical dashed line indicates the transition from Phases I to II of the bloom. The top graph shows changes in the tracer layer depths (z_{tl}), indicating the bottom depth of the IN-patch.

Table 4
Comparsion of bloom conditions and phytoplankton biomass properties during Fe enrichment experiments performed in HNLC regions of the Southern, Equatorial Pacific and North Pacific oceans

HNLC region	Mixed layer depth (m)	Bloom longevity[a] (d)	chl *a* ($mg\,m^{-3}$)		Integrated chl a[a] ($mg\,m^{-2}$)		Microphytoplankton (>20 μm) (% chl *a*)		Most abundant large diatoms[g]	References
			Initial	Peak[b]	Initial$_{(\int m)}$[c]	Peak$_{(\int m)}$	Initial	Peak		
Southern Ocean										
SOIREE (1999)	20–65	>40[d]	0.25–0.30	1.8	$20_{(65)}$	$115_{(65)}$	30	50	*Fragilariopsis kerguelensis*, *Thalassiosira* spp., *Rhizosolenia* spp.	Boyd et al., 2000; Gall et al., 2001a
EisenEx (2000)	40–80	>21[e]	0.6	2.8	$48–56_{(100)}$	$231_{(100)}$	10	45	*Pseudo-nitzschia* spp.	Gervais et al., 2002
SOFeX (2002)										
North Patch—Low $Si(OH)_4$	40	30	0.2	2.3	16.2	69.4	6	66	*Pseudo-nitzschia* spp.	D. Barber and W.O. Smith, unpubl. data
South Patch—High $Si(OH)_4$	50	18	0.25	3.9	23.2	88.7	48	57	*Fragilariopsis* sp., *Corethron* sp., *Chaetoceros* sp., *Rhizosolenia* sp.	
Equatorial Pacific										
IronEx II (1995)	25–50	7	0.15–0.20	3	$10_{(35)}$[f]	$100_{(35)}$[f]	10	60	*Nitzschia* spp., *Chaetoceros* spp.	Coale et al., 1996; Landry et al., 2000 Cavender-Bares et al., 1999
North Pacific										
Northwest—SEEDS (2001)	9–18	>13[e]	0.59–0.94	17.7	$36.2_{(50)}$	$342_{(50)}$	36	95	*Chaetoceros debilis*, *Pseudo-nitzschia turgidula*	Tsuda et al., 2003; S. Takeda, unpubl. data.
Northeast—SERIES (2002)	6–32	18	0.27–0.43	6.3	$14_{(46)}$	$114_{(25)}$	25	86	*Pseudo-nitzschia* spp., *Neodenticula* sp.,	This study

[a]Bloom longevity is defined as the number of days to reach and maintain maximum chlorphyll *a* concentrations in the patch.
[b]Measurement of the maximum chlorophyll *a* concentration in the patch.
[c]Denotes depth of chlorophyll *a* integration.
[d]Bloom longevity estimated from observed sea-surface chlorophyll *a* satellite data.
[e]Patch chlorophyll *a* was still increasing by the end of the denoted observation period.
[f]Approximate values calculated from vertical profiles provided in Coale et al., 1996.
[g]Major diatom species as determined by relative abundance at peak chlorophyll a concentrations in the patch.

in temporal evolution among experiments may be attributed to the range of temperatures between the cold polar, moderate subpolar and warm tropical waters (Boyd, 2002). During SOIREE, maximum net growth rates of microphytoplankton calculated from changes in chl *a* ranged between 0.15 and $0.2\,d^{-1}$ (Gall et al., 2001b). Equivalent calculations for microphytoplankton in SERIES yielded maximum net growth rates of $0.25–0.30\,d^{-1}$. It should be noted that estimates of net growth rates based on changes in chl *a* are usually lower than specific growth rates of the phytoplankton assemblage due to the potential reduction of phytoplankton biomass independent of cell physiology (i.e. patch dilution and zooplankton grazing). However, as previously mentioned, intense grazing on diatoms by macrozooplankton was not evident during SERIES. Moreover, shipboard "grow-out" experiments performed during SEEDS investigating the effects of temperature on phytoplankton growth and composition showed an increase in net growth rates of phytoplankton with elevated incubation temperature (Noiri et al., 2005). Thus, the growth rates of phytoplankton and the subsequent duration of the Fe-induced bloom may be strongly influenced by regional temperatures. The effects of dilution on patch evolution and biogeochemical processes during SERIES are discussed in Law et al. (this issue) and Timothy et al. (this issue).

The production of Fe-binding ligands may also contribute to bloom longevity. In SOIREE, the sharp increase in organic ligands from days 12 to 14 of the experiment was suggested to have maintained a pool of dissolved Fe (Maldonado et al., 2001). Henceforth, Fe bound to these ligands was suggested to regulate Fe uptake rates and phytoplankton growth. In contrast, during the SERIES experiment, Fe concentrations decreased rapidly from the patch, returning to ambient levels by day 13 (Boyd et al., 2004). This return to low Fe concentrations, along with $Si(OH)_4$ depletion, is believed to have contributed to the SERIES bloom termination.

A comparison in floristic shifts and size-classes of phytoplankton contributing to each Fe-stimulated assemblage identifies some similarities and differences among HNLC regions. In SERIES, there were significant initial increases in abundances of picophytoplankton, nanophytoplankton, and microphytoplankton, as observed in the other Fe enrichment experiments. Although diatoms appeared to dominate the final phytoplankton composition, the extent of diatom dominance differed among experiments. In the Southern polar region, the initially rare diatoms clearly exhibited the greatest response to Fe, yet final chl *a* concentrations were equally distributed between diatom and non-diatom phytoplankton species. Conversely, during SERIES and SEEDS, microphytoplankton comprised 86% and 95%, respectively, of total chl *a*. Therefore, the final algal composition in post-Fe enrichments is likely to be influenced by a number of factors, including initial phytoplankton assemblage, specific growth rates, selective grazing pressures and other limiting variables such as light and macronutrients. As these factors often vary both spatially and temporally, each subsequent Fe enrichment event may yield a different phytoplankton assemblage. Because different phytoplankton groups have distinct physiological and biochemical attributes, shifts in phytoplankton species composition may differentially influence coupled biogeochemical processes such as nutrient cycling, C export and sea-to-air gas exchange.

4.4. Diatom carbon export potential

The fate of an Fe-induced phytoplankton bloom is highly dependent on the size and species composition of the enhanced particulate organic matter, its ability to exit the euphotic zone and the resulting transformation of such particles in transit to the deep ocean (Boyd and Newton, 1995). These factors will determine the efficiency of the transport of photosynthetically fixed C from the surface to ocean depths, i.e. the biological pump (Volk and Hoffert, 1985). In many open ocean regions where diatoms make up a small fraction of the phytoplankton biomass, sediment trap analyses provides evidence that these large cells contribute a high proportion to downward PC fluxes (Boyd and Newton, 1999). Diatoms are effective transporters of C out of the euphotic zone due to their fast rates of sinking and slower rates of remineralization when compared to other algal groups (Buesseler, 1998). Among diatom genera, there exists a wide range of sizes and cellular elemental compositions that drastically influences their capacity as potential vectors for C export. Therefore, a detailed assessment of the change in phytoplankton species, as well as their elemental composition, is required to fully elucidate their C export potential.

With respect to the second tenet of the Fe hypothesis (the influence of marine primary productivity

on global climate), determining the extent of C sequestration during an Fe-induced bloom is critical. During SERIES, the concomitant increase in PC and chl *a* concentrations in the patch clearly portrayed the enhancement of C export potential. Similarly, export fluxes of PC, primarily composed of diatoms to depths below the patch, were clearly evident 24 days after the first Fe enrichment (Boyd et al., 2004). Due to the large range in cellular chl *a* and C contents among diatoms, cell abundance may not be a good indicator of C export potential. Therefore, C biovolume is a more applicable measure of a particular diatom's ability to sequester C. During SERIES, the large centric diatoms *Rhizosolenia* and *Probiscia*, as well as the large pennate diatom *Thalassiothrix*, did not dominate the bloom numerically. However, since these diatoms are much larger than *Pseudo-nitzschia*, *Neodenticula* and *Chaetoceros*, these large diatoms did comprise a significant amount of algal C. Thus, although pennate diatoms were most abundant, when peak populations of major diatom genera were converted to biovolume, centric diatoms contributed the majority of algal C to the bloom.

5. Summary

The outcome of SERIES confirmed that alleviation of Fe limitation in the NE subarctic Pacific during summer months results in an increase in phytoplankton biomass and a shift in assemblage from pico- and nanophytoplankton to large diatoms. The first ecological phase of the phytoplankton bloom began with an increase in growth of all phytoplankton size-classes as well as a decrease in PC: chl *a* ratios in both small ($<5\,\mu m$) and large ($\geqslant 5\,\mu m$) cells. By day 10, smaller phytoplankton size-classes had peaked with picophytoplankton dominated by *Synechococcus* spp. and nanophytoplankton dominated by Prymnesiophyceae (including coccolithophorids). In the second phase, both the biomass and abundance of smaller phytoplankton decreased rapidly, whereas microphytoplankton biomass continued to increase up to day 18. At this time, PC: chl *a* ratios in the small cells increased markedly, whereas in the large cells, PC: chl *a* ratios continued to decrease. Although pennate diatoms, such as *Pseudo-nitzschi*a spp. and *N. seminae* were most numerically dominant, when converted to biovolume, centric diatoms contributed the majority of the algal C biomass during the bloom. The enhanced phytoplankton biomass, primarily within fast-sinking diatoms, suggests an increased capacity for C sequestration by Fe enrichment, although the long-term fate of this C remains uncertain.

Acknowledgements

The authors would like to thank the scientists on board the CCGS *J.P Tully*, the *El Puma* and the *Kaiyo Maru* who were instrumental in carrying out sampling and data analyses during SERIES. In particular, we would like to thank B. Imanian and M. Guo for assistance with sample analyses. Light data were kindly provided by L. Ziolkowski from Dalhousie University and F. Whitney of the Institute of Ocean Sciences, Sidney BC. Tracer layer depths were kindly provided by C. Law from the National Institute of Water and Atmospheric Research, New Zealand and M. Arychuk from IOS. We are grateful to the officers and crew of the CCGS *J.P. Tully*, the *El Puma* and the *Kaiyo Maru* for their efforts at sea. This work is a contribution of the Canadian-SOLAS Network (Surface Ocean—Lower Atmosphere Study) funded by the Natural Sciences and Engineering Research Council of Canada (NSERC), the Canadian Foundation for Climate and Atmospheric Sciences (CFCAS), the Department of Fisheries and Oceans Canada, and the Department of Environment Canada.

References

Bishop, J.K.B., Davis, R.E., Sherman, J.T., 2002. Robotic observations of dust storm enhancement of carbon biomass in the North Pacific. Science 298, 817–821.

Booth, B.C., Lewin, J., Postel, J.R., 1993. Temporal variation in the structure of autotrophic and heterotrophic communities in the subarctic Pacific. Progress in Oceanography 31, 57–99.

Boyd, P.W., 2002. The role of iron in the biogeochemistry of the Southern Ocean and equatorial Pacific: a comparison of in situ iron enrichments. Deep-Sea Research II 49, 1803–1821.

Boyd, P., Harrison, P.J., 1999. Phytoplankton dynamics in the NE subarctic Pacific. Deep-Sea Research II 46, 2405–2432.

Boyd, P.W., Newton, P., 1995. Evidence of the potential influence of planktonic community structure on the interannual variability of particulate organic carbon flux. Deep-Sea Research I 42, 619–639.

Boyd, P.W., Newton, P.P., 1999. Does planktonic community structure determine downward particulate organic carbon flux in different oceanic provinces? Deep-Sea Research I 46, 63–91.

Boyd, P.W., Strom, S., Whitney, F.A., Doherty, S., Wen, M.E., Harrison, P.J., Wong, C.S., Varela, D.E., 1995. The NE subarctic Pacific in winter: I. Biological standing stocks. Marine Ecology Progress Series 128, 11–24.

Boyd, P.W., Muggli, D.L., Varela, D.E., Goldblatt, R.H., Chretien, R., Orians, K.J., Harrison, P.J., 1996. *In vitro* iron enrichment experiments in the NE subarctic Pacific. Marine Ecology Progress Series 136, 179–193.

Boyd, P.W., Wong, C.S., Merrill, J., Whitney, F., Snow, J., Harrison, P.J., Gower, J., 1998. Atmospheric iron supply and enhanced vertical carbon flux in the NE subarctic Pacific: is there a connection? Global Biogeochemical Cycles 12, 429–441.

Boyd, P.W., Watson, A.J., Law, C.S., Abraham, E.R., Trull, T., Murdoch, R., Bakker, D.C.E., Bowie, A.R., Buesseler, K.O., Chang, H., Charette, M., Croot, P., Downing, K., Frew, R., Gall, M., Hadfield, M., Hall, J., Harvey, M., Jameson, G., La Roche, J., Liddicoat, M., Ling, R., Maldonado, M.T., McKay, R.M., Nodder, S., Pickmere, S., Pridmore, R., Rintoul, S., Safi, K., Sutton, P., Strzepek, R., Tanneberger, K., Turner, S., Waite, A., Zeldis, J., 2000. A mesoscale phytoplankton bloom in the polar Southern Ocean stimulated by iron fertilization. Nature 407, 695–702.

Boyd, P.W., Law, C.S., Wong, C.S., Nojiri, Y., Tsuda, A., Levasseur, M., Takeda, S., Rivkin, R., Harrison, P.J., Strzepek, R., Gower, J., McKay, R.M., Abraham, E., Arychuk, M., Barwell-Clarke, J., Crawford, W., Crawford, D., Hale, M., Harada, K., Johnson, K., Kiyosawa, H., Kudo, I., Marchetti, A., Miller, W., Needoba, J., Nishioka, J., Ogawa, H., Page, J., Robert, M., Saito, H., Sastri, A., Sherry, N., Soutar, T., Sutherland, N., Taira, Y., Whitney, F., Wong, S.K.E., Yoshimura, T., 2004. The decline and fate of an iron-induced subarctic phytoplankton bloom. Nature 428, 549–553.

Buesseler, K.O., 1998. The decoupling of production and particulate export in the surface. Global Biogeochemical Cycles 12, 297–310.

Cavender-Bares, K.K., Mann, E.L., Chisholm, S.W., Ondrusek, M.E., Bidigare, R.R., 1999. Differential response of equatorial Pacific phytoplankton to iron fertilization. Limnology and Oceanography 44, 237–246.

Coale, K.H., 1991. Effects of iron, manganese, copper, and zinc enrichments on productivity and biomass in the sub-Arctic Pacific. Limnology and Oceanography 36, 1851–1864.

Coale, K.H., Johnson, K.S., Fitzwater, S.E., Gordon, R.M., Tanner, S., Chavez, F.P., Ferioli, L., Sakamoto, C., Rogers, P., Millero, F., Steinberg, P., Nightingale, P., Cooper, D., Cochlan, W.P., Landry, M.R., Constantinou, J., Rollwagen, G., Trasvina, A., Kudela, R., 1996. A massive phytoplankton bloom induced by an ecosystem-scale iron fertilization experiment in the equatorial Pacific Ocean. Nature 383, 495–501.

Coale, K.H., Johnson, K.S., Chavez, F.P., Buesseler, K.O., Barber, R.T., Brzezinski, M.A., Cochlan, W.P., Millero, F.J., Falkowski, P.G., Bauer, J.E., Wanninkhof, R.H., Kudela, R.M., Altabet, M.A., Hales, B.E., Takahashi, T., Landry, M.R., Bidigare, R.R., Wang, X.J., Chase, Z., Strutton, P.G., Friederich, G.E., Gorbunov, M.Y., Lance, V.P., Hilting, A.K., Hiscock, M.R., Demarest, M., Hiscock, W.T., Sullivan, K.F., Tanner, S.J., Gordon, R.M., Hunter, C.N., Elrod, V.A., Fitzwater, S.E., Jones, J.L., Tozzi, S., Koblizek, M., Roberts, A.E., Herndon, J., Brewster, J., Ladizinsky, N., Smith, G., Cooper, D., Timothy, D., Brown, S.L., Selph, K.E., Sheridan, C.C., Twining, B.S., Johnson, Z.I., 2004. Southern ocean iron enrichment experiment: carbon cycling in high- and low-Si waters. Science 304, 408–414.

Conway, H.L., Harrison, P.J., 1977. Marine diatoms grown in chemostats under silicate or ammonium limitation 4. Transient response of *Chaetoceros debilis*, *Skeletonema costatum*, and *Thalassiosira gravida* to a single addition of limiting nutrient. Marine Biology 43, 33–43.

Cullen, J.J., 1995. Status of the iron hypothesis after the open-ocean enrichment experiment. Limnology and Oceanography 40, 1336–1343.

Fung, I.Y., Meyn, S.K., Tegen, I., Doney, S.C., John, J.G., Bishop, J.K.B., 2000. Iron supply and demand in the upper ocean. Global Biogeochemical Cycles 14, 281–295.

Gall, M.P., Boyd, P.W., Hall, J., Safi, K.A., Chang, H., 2001a. Phytoplankton processes. Part 1: community structure during the Southern Ocean iron RElease experiment (SOIREE). Deep-Sea Research II 48, 2551–2570.

Gall, M.P., Strzepek, R., Maldonado, M., Boyd, P.W., 2001b. Phytoplankton processes. Part 2. Rates of primary production and factors controlling algal growth during the Southern Ocean Iron RElease experiment (SOIREE). Deep-Sea Research II 48, 2571–2590.

Geider, R.J., La Roche, J., Greene, R., Olaizola, M., 1993. Response of the photosynthetic apparatus of *Phaeodactylum tricornutum* (Bacillariophyceae) to nitrate, phosphate or iron limitation. Journal of Phycology 29, 755–766.

Gervais, F., Riebesell, U., Gorbunov, M.Y., 2002. Changes in primary productivity and chlorophyll a in response to iron fertilization in the Southern Polar Frontal Zone. Limnology and Oceanography 47, 1324–1335.

Greene, R.M., Geider, R.J., Kolber, Z., Falkowski, P.G., 1992. Iron-induced changes in light harvesting and photochemical energy-conversion processes in eukaryotic Marine-Algae. Plant Physiology 100, 565–575.

Hale, M.S., Rivkin, R.B., Matthews, P., Agawin, N.S.R., Li, W.K.W., this issue. Microbial response to a mesoscale iron enrichment in the NE subarctic Pacific: heterotrophic bacterial processes. Deep-Sea Research II.

Hasle, G.R., Fryxell, G.A., 1970. Diatoms, cleaning and mounting for light and electron microscopy. Transactions of the American Microscopical Society 89, 469–474.

Johnson, K.S., Gordon, R.M., Coale, K.H., 1997. What controls dissolved iron concentrations in the world ocean? Marine Chemistry 57, 137–161.

Johnson, W.K., Miller, L.A., Sutherland, A.E., Wong, C.S., 2005. Iron transport by mesoscale Haida eddies in the Gulf of Alaska. Deep-Sea Research II 52, 933–953.

Landry, M.R., Ondrusek, M., Tanner, S., Brown, S.L., Constantinou, J., Bidigare, R., Coale, K.H., Fitzwater, S., 2000. Biological response to iron fertilization in the eastern equatorial Pacific (IronEx II). I. Microplankton community abundances and biomass. Marine Ecology Progress Series 201, 27–42.

Law, C. S., Crawford, W. R., Smith, M. J., Boyd, P. W., Wong, C. S., Nojiri, Y., Arychuck, M., Robert, M., Abraham, E. R., Johnson, W. K., Forsland, V., this issue. Patch evolution and the biogeochemical impact of entrainmnent during an iron fertilisation experiment in the Sub-Arctic Pacific. Deep-Sea Research II, doi:10.1016/j.dsr2.2006.05.028.

Maldonado, M.T., Boyd, P.W., La Roche, J., Strzepek, R., Waite, A., Bowie, A.R., Croot, P.L., Frew, R.D., Price, N.M., 2001. Iron uptake and physiological response of phytoplankton during a mesoscale Southern Ocean iron enrichment. Limnology and Oceanography 46, 1802–1808.

Marchetti, A., Juneau, P., Whitney, F.A., Wong, C.S., Harrison, P.J., this issue-a. Phytoplankton processes during a mesoscale Fe enrichment in the NE subarctic Pacific: Part II—nutrient utilization. Deep-Sea Research II, doi:10.1016/j.dsr2.2006.05.031.

Marchetti, A., Sherry, N.D., Juneau, P., Strzepek, R.F., Harrison, P.J., this issue-b. Phytoplankton processes during a mesoscale Fe enrichment in the NE subarctic Pacific: Part III—primary productivity. Deep-Sea Research II, doi:10.1016/j.dsr2.2006.05.032.

Martin, J.H., 1990. Glacial-interglacial CO_2 change: the iron hypothesis. Paleoceanography 5, 1–13.

Martin, J.H., Fitzwater, S., 1988. Iron deficiency limits phytoplankton growth in the north-east Pacific subarctic. Nature 331, 341–343.

Martin, J.H., Gordon, R.M., Fitzwater, S., Broenkow, W.W., 1989. Vertex—phytoplankton iron studies in the Gulf of Alaska. Deep-Sea Research I 36, 649–680.

Martin, J.H., Broenkow, W.W., Fitzwater, S.E., Gordon, R.M., 1990. Does iron really limit phytoplankton production in the offshore sub-Arctic Pacific—yes, it does—a reply. Limnology and Oceanography 35, 775–777.

Martin, J.H., Gordon, R.M., Fitzwater, S.E., 1991. The case for iron. Limnology and Oceanography 36, 1793–1802.

Martin, J.H., Coale, K.H., Johnson, K.S., Fitzwater, S.E., Gordon, R.M., Tanner, S.J., Hunter, C.N., Elrod, V.A., Nowicki, J.L., Coley, T.L., Barber, R.T., Lindley, S., Watson, A.J., Vanscoy, K., Law, C.S., Liddicoat, M.I., Ling, R., Stanton, T., Stockel, J., Collins, C., Anderson, A., Bidigare, R., Ondrusek, M., Latasa, M., Millero, F.J., Lee, K., Yao, W., Zhang, J.Z., Friederich, G., Sakamoto, C., Chavez, F., Buck, K., Kolber, Z., Greene, R., Falkowski, P., Chisholm, S.W., Hoge, F., Swift, R., Yungel, J., Turner, S., Nightingale, P., Hatton, A., Liss, P., Tindale, N.W., 1994. Testing the iron hypothesis in ecosystems of the Equatorial Pacific Ocean. Nature 371, 123–129.

Montagnes, D.J.S., Berges, J.A., Harrison, P.J., Taylor, F.J.R., 1994. Estimating carbon, nitrogen, protein, and chlorophyll *a* from volume in marine phytoplankton. Limnology and Oceanography 39, 1044–1060.

Morel, F.M.M., 1987. Kinetics of nutrient uptake and growth in phytoplankton. Journal of Phycology 23, 137–150.

Morel, F.M.M., Hudson, R.J.M., Price, N.M., 1991. Iron nutrition of phytoplankton and its possible importance in the ecology of ocean regions with high nutrient and low biomass. Oceanography 4, 56–61.

Nelson, D.M., Dortch, Q., 1996. Silicic acid depletion and silicon limitation in the plume of the Mississippi River: evidence from kinetic studies in spring and summer. Marine Ecology Progress Series 62, 283–292.

Nelson, D.M., Brzezinski, M.A., Sigmon, D.E., Franck, V.M., 2001. A seasonal progression of Si limitation in the Pacific sector of the Southern Ocean. Deep-Sea Research II 48, 3973–3995.

Noiri, Y., Kudo, I., Kiyosawa, H., Tsuda, A., 2005. Iron and temperature, two factors influencing phytoplankton species composition in the Western subarctic Pacific Ocean. Progress in Oceanography 64, 149–166.

Price, N.M., Ahner, B.A., Morel, F.M.M., 1994. The Equatorial Pacific-Ocean—Grazer-controlled phytoplankton populations in an iron-limited ecosystem. Limnology and Oceanography 39, 520–534.

Sastri, A.R., Dower, J.F., this issue. Mesozooplankton community response during the SERIES iron enrichment experiment in the subarctic NE Pacific. Deep-Sea Research II, doi:10.1016/j.dsr2.2006.05.034.

Sunda, W., Huntsman, S.A., 1995. Iron uptake and growth limitation in oceanic and coastal phytoplankton. Marine Chemistry 50, 189–206.

Sunda, W.G., Huntsman, S.A., 1997. Interrelated influence of iron, light and cell size on marine phytoplankton growth. Nature 390, 389–392.

Sunda, W.G., Swift, D.G., Huntsman, S.A., 1991. Low iron requirement for growth in oceanic phytoplankton. Nature 351, 55–57.

Timothy, D.A., Wong, C.S., Nojiri, Y., Ianson, D.C., Whitney, F.A. The effects of patch expansion on budgets of C, N and Si for the Subarctic Ecosystem Response to Iron Enrichment Study (SERIES). Deep-Sea Research II, this issue, doi:10.1016/j.dsr2.2006.05.042.

Tsuda, A., Takeda, S., Saito, H., Nishioka, J., Nojiri, Y., Kudo, I., Kiyosawa, H., Shiomoto, A., Imai, K., Ono, T., Shimamoto, A., Tsumune, D., Yoshimura, T., Aono, T., Hinuma, A., Kinugasa, M., Suzuki, K., Sohrin, Y., Noiri, Y., Tani, H., Deguchi, Y., Tsurushima, N., Ogawa, H., Fukami, K., Kuma, K., Saino, T., 2003. A mesoscale iron enrichment in the western subarctic Pacific induces a large centric diatom bloom. Science 300, 958–961.

Tsuda, A., Kiyosawa, H., Kuwata, A., Mochizuki, M., Naonobu, S., Saito, H., Chiba, S., Imai, K., Nishioka, J., Ono, T., 2005. Responses of diatoms to iron-enrichment (SEEDS) in the western subarctic Pacific, temporal and spatial comparisons. Progress in Oceanography 64, 189–205.

Volk, T., Hoffert, M.I., 1985. Ocean carbon pumps: analysis of relative strengths and efficiencies in ocean-driven atmospheric CO_2 changes. Geophysical Monographs 32, 99–110.

Whitney, F.A., Freeland, H.J., 1999. Variability in upper-ocean water properties in the NE Pacific Ocean. Deep-Sea Research I 46, 2351–2370.

Whitney, F.A., Crawford, D.W., Yoshimura, T., 2005. The uptake and export of Si and N in HNLC waters of the NE Pacific. Deep-Sea Research II 52, 1055–1067.

Wong, C.S., Matear, R.J., 1999. Sporadic silicate limitation of phytoplankton productivity in the subarctic NE Pacific. Deep-Sea Research II 46, 2539–2555.